

# PI3K inhibitors protect against glucocorticoid-induced skin atrophy

Shivani Agarwal <sup>a</sup>, Salida Mirzoeva <sup>a</sup>, Ben Readhead <sup>b</sup>, Joel T. Dudley <sup>c</sup>, Irina Budunova <sup>a,\*</sup>

<sup>a</sup> Department of Dermatology, Feinberg School of Medicine, Northwestern University, Chicago, IL, USA

<sup>b</sup> ASU-Banner Neurodegenerative Disease Research Center, Arizona State University, Tempe, AZ, USA

<sup>c</sup> Institute for Next Generation Healthcare, Department of Genetics and Genomic Sciences, Icahn School of Medicine at Mount Sinai, New York, NY, USA



## ARTICLE INFO

### Article history:

Received 29 October 2018

Received in revised form 16 January 2019

Accepted 17 January 2019

Available online 5 February 2019

### Keywords:

Glucocorticoid receptor

REDD1

FKBP51

Skin atrophy

PI3K/mTOR/Akt inhibitor

mTOR

## ABSTRACT

**Background:** Skin atrophy is a major adverse effect of topical glucocorticoids. We recently reported that REDD1 (regulated in development and DNA damage 1) and FKBP51 (FK506 binding protein 5), negative regulators of mTOR/Akt signaling, are induced by glucocorticoids in mouse and human skin and are central drivers of steroid skin atrophy. Thus, we hypothesized that REDD1/FKBP51 inhibitors could protect skin against catabolic effects of glucocorticoids.

**Methods:** Using drug repurposing approach, we screened LINCS library (<http://lincsproject.org/LINCS/>) to identify repressors of REDD1/FKBP51 expression. Candidate compounds were tested for their ability to inhibit glucocorticoid-induced REDD1/FKBP51 expression in human primary/immortalized keratinocytes and in mouse skin. Reporter gene expression, microarray, and chromatin immunoprecipitation were employed to evaluate effect of these inhibitors on the glucocorticoid receptor (GR) signaling.

**Findings:** Bioinformatics analysis unexpectedly identified phosphoinositide-3-kinase (PI3K)/mTOR/Akt inhibitors as a pharmacological class of REDD1/FKBP51 repressors. Selected PI3K/mTOR/Akt inhibitors—Wortmannin (WM), LY294002, AZD8055, and two others indeed blocked REDD1/FKBP51 expression in human keratinocytes. PI3K/mTOR/Akt inhibitors also modified global effect of glucocorticoids on transcriptome, shifting it towards therapeutically important transrepression; negatively impacted GR phosphorylation; nuclear translocation; and GR loading on REDD1/FKBP51 gene promoters. Further, topical application of LY294002 together with glucocorticoid fluocinolone acetonide (FA) protected mice against FA-induced proliferative block and skin atrophy but did not alter the anti-inflammatory activity of FA in ear edema test.

**Interpretation:** Our results built a strong foundation for development of safer GR-targeted therapies for inflammatory skin diseases using combination of glucocorticoids with PI3K/mTOR/Akt inhibitors.

**Fund:** Work is supported by NIH grants R01GM112945, R01AI125366, and HESI-THRIVE foundation.

© 2019 Published by Elsevier B.V. This is an open access article under the CC BY-NC-ND license (<http://creativecommons.org/licenses/by-nc-nd/4.0/>).

## 1. Introduction

Glucocorticoid hormones are important regulators of proliferation, differentiation, inflammation, and metabolism in skin [1,2]. Interestingly, many studies have now established that skin cells possess the complete biochemical machinery for efficient steroidogenesis including

**Abbreviations:** GR, Glucocorticoid receptor; GRE, glucocorticoid responsive element; FA, Fluocinolone acetonide; WM, Wortmannin; FKBP51, FK506-binding protein; ChIP, Chromatin immunoprecipitation; CO, croton oil; DDIT4, DNA damage inducible transcript 4; DEG, differentially expressed gene; 4EBP1, eukaryotic initiation factor 4E binding protein 1; FC, fold change; mTOR, mammalian target of Rapamycin; NF- $\kappa$ B, nuclear factor kappa B; REDD1, regulated in development and DNA damage response 1; rpS6, ribosomal protein S6; SEGRAM, selective glucocorticoid receptor agonist or modulator; TA, transactivation; TF, transcription factor; TR, transrepression.

\* Corresponding author at: Department of Dermatology, Northwestern University, Ward Building 9-132, 303 East Chicago Avenue, Chicago, IL 60611, USA.

E-mail address: [i-budunova@northwestern.edu](mailto:i-budunova@northwestern.edu) (I. Budunova).

synthesis of GCs, starting from the cholesterol biosynthesis [3–6]. Moreover, the reduced level of endogenous GCs have been causatively linked to the development of cutaneous diseases, including psoriasis [2]. The synthetic glucocorticoids (GCs) were introduced to the clinic from 1950s, and are still among the most widely used and efficient drugs for systemic and topical therapies of inflammatory and autoimmune visceral and dermatological diseases, such as atopic dermatitis/eczema and psoriasis [7]. Unfortunately, chronic treatment with GCs results in numerous adverse metabolic and atrophic effects including osteoporosis, muscle waste, skin atrophy [8,9].

The effects of glucocorticoids are mediated by the glucocorticoid receptor (GR), a known transcription factor (TF). In non-activated cells, GR resides in the cytoplasm bound to the molecular chaperones: heat shock proteins and immunophilins [10]. Upon hormone binding, GR undergoes phosphorylation and translocates to the nucleus, where it regulates gene expression positively (transactivation, TA) or negatively (transrepression, TR). TA is triggered mainly via binding of GR

## Research in context

### Evidence before this study

Millions of patients are affected by chronic inflammatory diseases, including dermatological diseases such as atopic dermatitis and psoriasis. The glucocorticoids (GCs) are among the most effective and frequently prescribed anti-inflammatory drugs. Unfortunately, chronic use of GCs is associated with numerous adverse effects such as altered glucose metabolism, steroid-induced diabetes, osteoporosis, impaired wound healing, skin and muscle atrophy. Skin atrophy is one of the major adverse effects of topical glucocorticoids, it affects all skin compartments: epidermis, dermis, dermal adipose, and as a result, significantly weakens the barrier function of the skin. We recently identified two mTOR/Akt inhibitors: REDD1 (Regulated in Development and DNA Damage 1) and FKBP51 (FK506-Binding Protein-51) as central drivers of steroid-induced skin atrophy. Indeed, in animals lacking either FKBP51 or REDD1, all skin compartments and skin stem cells were significantly protected against steroid hypoplasia. Thus, we hypothesized that dual REDD1/FKBP51 inhibitors could act as anti-atrophic compounds and could be combined with GCs for tissue protection during chronic treatments.

### Added value of this study

Inhibitors of REDD1 and FKBP51 expression were selected using a drug repurposing approach, via bioinformatics screening of LINCS database comprised of transcriptional signatures induced by FDA-approved and experimental drugs (<http://lincsproject.org/LINCS/>). We identified phosphoinositide-3-kinase (PI3K)/mTOR/Akt inhibitors as the most prominent pharmacological class of the repurposing candidates. Since PI3K/ mTOR/Akt inhibitors were developed as anti-cancer drugs, and are known for their ability to inhibit cell proliferation, their potential to alleviate development of steroid-induced skin atrophy was unexpected. We selected five compounds, including wortmannin (WM), LY294002, and AZD8055 for experimental validation of their effects on REDD1 and FKBP51 expression, glucocorticoid receptor (GR) function, and on therapeutic (anti-inflammatory) and adverse (skin atrophy) effects of glucocorticoids. We experimentally proved that all tested compounds blocked REDD1 and FKBP51 expression in human primary and immortalized HaCaT keratinocytes and in mouse skin. We also discovered that PI3K/mTOR/Akt inhibitors modified glucocorticoid receptor (GR) function by shifting its activity towards therapeutically important transrepression (negative gene regulation). The underlying molecular mechanisms include inhibition of GR phosphorylation, nuclear translocation, and GR loading onto the gene promoters of atrophogenes, as well as inhibition of NF- $\kappa$ B. Most importantly, topical application of LY294002 (in the special formulation to increase penetration through epidermal barrier) together with glucocorticoid flucinolone acetonide (FA) protected mice against FA-induced proliferative block and skin atrophy but did not alter the anti-inflammatory activity of FA.

### Implications of all the available evidence

Our novel observations that PI3K/mTOR/Akt inhibitors beneficially modified GR activity at the global level, could explain the improved therapeutic index of glucocorticoids (benefit to risk ratio) when they were combined with these inhibitors. Overall, our studies

support the development of innovative safer GR-targeted therapies with glucocorticoids using REDD1/FKBP51 inhibitors as tissue protectors against steroid-induced atrophy. Our findings have important clinical implications for skin diseases but also for various visceral inflammatory diseases treated with GCs as they induce atrophy in different tissues including muscle and bone.

homodimers to glucocorticoid-responsive elements (GRE) in gene promoters and enhancers. TR is mediated by different mechanisms including negative protein-protein interaction between GR and other TFs such as pro-inflammatory factors NF- $\kappa$ B and AP-1 [11–14].

It has been long established that GR TR is important for anti-inflammatory activity of GCs (therapeutic effects). At the same time, many side effects that reflect catabolic activity of GCs (such as osteoporosis, skin and muscle atrophy) primarily are linked to the TA branch of GR signaling [8,9,15,16]. Thus, for years the major efforts in the field have been focused on the development of selective GR agonists and modulators (SEGRAM) that shift GR activity towards TR [9]. However, only few SEGRAMs have reached clinical trials, and there is still a need for safer GR-targeted anti-inflammatory therapies. We proposed and tested here, in skin atrophy model, an alternative approach - a combination of GCs with compounds that can protect tissues against their atrophic side effects.

Skin atrophy is one of the most common serious side effects of topical GCs. Chronic GCs treatment results in drastic hypoplasia of all skin compartments, increased fragility, tearing, bruising, and defects in skin barrier function [17,18]. Our recent studies have led to the identification of GR target genes DDIT4 (DNA damage inducible transcript 4)/REDD1 (regulated in development and DNA damage response 1) and FKBP51 (FK506 binding protein 5) as central drivers of steroid-induced skin atrophy [12,18].

REDD1 is a nutrient/energy sensor and an early stress-response gene activated by hypoxia, depletion of growth factors, DNA damage as well as GCs [19–21]. FKBP51 is a member of the immunophilin protein family. It acts as a multi-client chaperone (GR is one of its best studied clients), and is involved in immunoregulation and basic cellular processes such as protein folding and trafficking [22,23]. Even though both genes have pleiotropic functions, they play similar roles in negative regulation of mTOR/Akt signaling. Full Akt activation requires phosphorylation at Thr308 and Ser473 [24–26]. FKBP51 enhances the interaction between phosphatases PHLPP1/2 and Akt, followed by Akt dephosphorylation at Ser473 [25,26]. In addition, FKBP51 can negatively inhibit mTOR via binding to its FK506-rapamycin binding domain [26,27]. At the same time, REDD1 promotes Akt dephosphorylation at Thr308 by protein phosphatase 2A (PP2A) [28], and can block mTOR activity via activation of TSC1/2 (tuberous sclerosis complexes 1/2) [29].

The fact that all the skin compartments (epidermis, dermis and dermal adipose) in REDD1 and FKBP51 knockout mice were significantly protected from the atrophic effects of GCs [12,18], suggested that dual REDD1/FKBP51 inhibitors could be used in combination with GCs as tissue protectors. To select REDD1/FKBP51 small molecule inhibitors we used drug repurposing approach and screened LINCS database of ~ 20,000 transcriptional signatures induced by FDA-approved and experimental drugs (<http://lincsproject.org/LINCS/>) focusing on their potential to block REDD1 and FKBP51 expression. Unexpectedly, we identified phosphoinositide-3-kinase (PI3K)/mTOR/Akt inhibitors as the most prominent pharmacological class of the repurposing candidates. We have chosen five compounds, including wortmannin (WM), LY294002, and AZD8055, for experimental validation of their effects on REDD1 and FKBP51 expression, GR function, evaluation of their effects on anti-inflammatory activity of GCs, and their protective anti-atrophogenic effects in murine skin chronically treated with steroids.

## 2. Materials and methods

### 2.1. Chemicals, reagents and antibodies

Fluocinolone acetonide (FA), croton oil (CO), Wortmannin (WM), AZD8055 (AZD), NVP-BEZ235 (NVP), MK-2206 (MK), and 5-bromo-2'-deoxyuridine (BrdU), were from Sigma Aldrich (St. Louis, MO), LY294002 (LY) was from LC Laboratories (Woburn, MA). TNF- $\alpha$  and cytoplasmic and nuclear fractionation kit were from Thermo Fisher Scientific (Waltham, MA).

We used antibodies to GR (sc-8992, RRID:AB\_2155784), RelA/p65 (sc-8008, RRID:AB\_628017), phospho-RelA/p65 (Ser536) (sc-136548, RRID:AB\_10610391), I $\kappa$ B (sc-1643, RRID:AB\_627772), phospho-I $\kappa$ B (Ser32) (sc-8404, RRID:AB\_627773), FKBP51 (sc-271547, RRID:AB\_10649040) (Santa Cruz Biotechnology, Dallas, TX); GAPDH (G9545, RRID:AB\_796208, Sigma Aldrich); phospho-GR (Ser211) (4161, RRID:AB\_2155797), phospho-rpS6 (Ser235/236) (4856S, RRID:AB\_2181037), phospho-4E-BP1 (Thr37/46) (9459L, RRID:AB\_2262165), phospho-P70S6K (Thr389) (9234, RRID:AB\_2269803), phospho-AKT (Thr308 and Ser473) (9266S, RRID:AB\_659801 and 9271, RRID:AB\_329825), lamin B (12586, RRID:AB\_2650517) and tubulin (2148, RRID:AB\_2288042) (Cell Signaling, San Jose, CA), REDD1 (10638-1-AP, RRID:AB\_2245711, Proteintech Group, Rosemont, IL).

### 2.2. Computational selection of REDD1/FKBP51 inhibitors

Small molecule inhibitors of REDD1/FKBP51 expression were identified by computational screening of LINCS library (<http://lincsproject.org/LINCS/>) comprised of the results of ~1 million experiments in which the global effect of >20,000 unique compounds on human cell transcriptome was accessed across 50 cell types of varied lineage using custom-made DNA arrays. The molecular signature of each compound in each experiment is presented at LINCS as a list of DEGs - differentially expressed genes (compound-treated versus solvent-treated), ordered by descending expression fold-change. The top putative REDD1 inhibitors were selected according to the number of LINC experiments in which REDD1 was within 100 most down-regulated genes in treated cells. Next, we selected among potential REDD1 inhibitors compounds that also inhibited FKBP51. For statistical computing, we used the R project version 3.2.5 (<https://www.r-project.org/>).

### 2.3. Cell cultures

Immortalized human keratinocyte cell line HaCaT was a kind gift of Dr. Kathleen J Green (Northwestern University, Chicago, IL). The cells were maintained in DMEM medium supplemented with 10% fetal bovine serum (FBS) and 100 U/mL penicillin, 100  $\mu$ g/mL streptomycin. Human epidermal keratinocytes (NHEK) derived from neonatal foreskin were obtained from Northwestern Skin Disease Research Center (SDRC) and cultured in M154 medium with added calcium (70  $\mu$ M) and growth supplements (all but hydrocortisone) from KGM™ Gold Keratinocyte Growth Medium BulletKit™ (Lonza, Basel, Switzerland).

### 2.4. Treatment of cells

Twenty-four hrs before the treatment, HaCaT cells were switched to phenol-free DMEM supplemented with 10% charcoal-stripped serum (Sigma Aldrich, St. Louis, MO) to deplete glucocorticoids in the cells. The inhibitors and FA were dissolved in DMSO; DMSO (<0.1%) was used as vehicle control in all the experiments unless otherwise stated.

Inhibitors WM (10  $\mu$ M), LY294002 (50  $\mu$ M), AZD8055 (1  $\mu$ M), NVP (1  $\mu$ M) and MK-2206 (5  $\mu$ M) were added to the culture medium 6 h prior to FA, and then cells were further cultivated for 24 h in the presence of FA and PI3K/mTOR/Akt inhibitors.

### 2.5. Luciferase Assay

Cells were transduced with lentiviruses expressing GRE-Luciferase, NF- $\kappa$ B-Luciferase or control mCMV-Luciferase, to generate the reporter cells. The viral stocks were obtained from the Northwestern University SDRC RNA/DNA delivery Core. Reporter cells were pretreated for 6 h with PI3K/mTOR/Akt inhibitors (10  $\mu$ M WM, 50  $\mu$ M LY294002 and 1  $\mu$ M AZD8055) or vehicle followed by FA (1  $\mu$ M) or vehicle treatment for 24 h. Luciferase activity was measured using a luminometer (TD-20/20) as described [12]. Fold change in luciferase expression was normalized to the total protein concentration in each sample.

### 2.6. Cell viability assay

HaCaT and NHEK cells ( $1 \times 10^5$  cells/well) were plated in 96 well plate and pretreated for 6 h with the inhibitors or vehicle control, followed by addition of FA (1  $\mu$ M) or vehicle. Twenty-four hrs later, MTT reagent (3-(4,5-dimethylthiazol-2-yl)-2,5-diphenyltetrazolium bromide) was added to wells, and plates were incubated for 4 h. Formazan product was dissolved in DMSO and absorbance was measured at 570 nm in a plate-reader.

### 2.7. Western blot analysis

Cell lysates were subjected to nuclear and cytosolic protein fractionation using NE-PER nuclear and cytoplasmic extraction reagents (Thermo Fisher Scientific). Proteins were resolved by SDS-PAGE and transferred to Odyssey nitrocellulose membranes (LI-COR Biosciences, Lincoln, NE). The membranes were blocked, incubated overnight at 4 °C with primary antibodies followed by IRDye® secondary antibodies (800CW conjugated Goat-anti-Rabbit and Donkey-anti-Mouse, Cat# 926-32211, RRID:AB\_621843 and Cat# 926-32212, RRID:AB\_621847) (LI-COR Biosciences). Immunoreactive signals were captured in digital format using LI-COR Odyssey imager. To normalize the protein expression, we used GAPDH and tubulin antibodies for the whole cell lysates and lamin B (LMNB1) antibodies for the nuclear fractions.

### 2.8. Real-time polymerase chain reaction (RT-PCR/Q-PCR)

RNA was extracted from cells using EZNA total RNA kit 1 (Omega BioTrek, Norcross, GA). Random hexamers, M-MLV reverse transcriptase (Thermo Fisher Scientific) and 1  $\mu$ g of total RNA were used for reverse transcription. The gene-specific primers were designed using the NCBI Primer-BLAST tool (<http://www.ncbi.nlm.nih.gov/tools/primer-blast/>) and their sequences were as described previously [30]. Q-PCR was performed with SsoAdvanced™ Universal SYBR Green Supermix (Bio-Rad Laboratories, Hercules, CA) [30]. The real-time RT-PCR reactions were carried out using Roche LightCycler® 480 system. Fold change was calculated as  $2^{-\Delta\Delta Ct}$  and the values were normalized to the housekeeping RPL27 transcript.

### 2.9. Immunofluorescence

HaCaT cells grown on glass slides were fixed and permeabilized as described [30]. Fixed cells were stained with anti-GR antibody (H-300, Santa Cruz Biotechnology, 1:500 dilution) and Alexa fluor®555 goat anti-rabbit IgG (Cat# A27039, RRID:AB\_2536100) (1:1000 dilution, Thermo Fisher Scientific). Nuclei were stained with Hoechst 33342 (1:10,000 dilution, Thermo Fisher Scientific). Cells were mounted using ProLong gold antifade mounting medium (Thermo Fisher Scientific) and images are taken with AxioCaM HRC camera linked with Zeiss Axioplan2 microscope. Images shown are representation of at least 10 images captured for each sample.

### 2.10. Chromatin immunoprecipitation (ChIP) analysis

HaCaT cells were treated with FA (1  $\mu$ M) in the presence or absence of WM (10  $\mu$ M) or LY294002 (50  $\mu$ M) for 24 h, as described above. Samples were processed using EMD Millipore EZ-Magna ChIP™ A/G kit (EMD Millipore, Burlington, MA), purified DNA was subjected to Q-PCR analysis and fold enrichments were calculated as described [30].

The GR binding sites in human REDD1 and FKBP51 promoters were predicted based on HOCOMOCO models of TF binding motifs that utilize ChIP-Seq and HT-SELEX data [31]. Primers used for ChIP for GREs in human REDD1 promoter region were as published previously [30] and for human FKBP51 gene promoter are listed in Supplemental Table S8. Results represent an average of three independent experiments and are quantified as described [30].

### 2.11. Microarray analysis of gene expression by Illumina BeadChip array

RNA was extracted from HaCaT keratinocytes treated with FA (1  $\mu$ M) in the presence or absence of LY294002 (50  $\mu$ M). The experiment was repeated twice. HumanHT-12, Whole-Genome Gene Expression BeadChip array (Illumina, San Diego, CA) was used for RNA labeling, amplification and hybridization at the University of Chicago Genomics Facility. Array results were submitted to NCBI (GSE120991). Microarray processing was performed using the Limma package [32]. The neqc function was used for background subtraction, and quantile normalization with both positive and negative control probes. Probes with adjusted P value (FDR) < 0.1 were considered differentially expressed probes/genes (DEG) and retained for further analysis. The results of microarray were validated by Q-PCR. Q-PCR and microarray based gene expression values were compared using linear Pearson correlation.

### 2.12. Molecular functional annotations and pathway analysis

Entrez identifiers for DEGs (FDR < 0.1) were used to identify gene set enrichments. We performed a Fisher's exact test to identify significant overlap between DEGs and each gene set. P-values were adjusted using the Benjamini & Hochberg method [33]. Gene sets enrichment analysis was done using the online tool of GSEA (Broad Institute, Cambridge, MA) with the GO molecular function and Hallmark database gene sets (<http://software.broadinstitute.org/gsea/msigdb/index.jsp>).

### 2.13. Computational analysis and visualization of microarray differential expression results

Computational analysis was performed using the R project version 3.2.5. R packages Ggplot2 [34] and Ggrepel (<http://github.com/slowkow/ggrepel>) were used to visualize global effect of LY294002 on FA-induced gene expression changes.

### 2.14. Ethics statement

All animal housing and experiments were performed according to the protocols approved by the Northwestern University Animal Care and Use Committee, in a strict adherence to the National Institutes of Health guidelines.

### 2.15. Animals and treatments

Experiments were performed on seven-week-old F1 C57BL/6  $\times$  129 female mice (Taconic, Germantown, NY) in the telogen stage of hair cycle to avoid variability that could be introduced by hair cycling [35]. Mice were shaved three days before the application of FA, 4 animals were used per treatment group.

### 2.16. Acute treatment

Animals were topically treated with 200  $\mu$ L of vehicle alone (30% PEG3350, 4% DMSO, 5% Tween 20 in PBS) or LY294002 (10 nmoles/mouse) in same vehicle for 5 h, and then treated with 200  $\mu$ L of acetone (vehicle control) or FA in acetone (1  $\mu$ g/mouse) for 8 h (for RNA and protein isolation) or for 24 h (for BrdU staining). Skin was harvested, and epidermis mechanically separated from dermis was used for RNA isolation as described [12]. BrdU (50  $\mu$ g/g body weight) was injected intraperitoneally 1 h before skin was harvested.

### 2.17. Skin atrophy test

Skin atrophy was induced by chronic topical FA treatment (1  $\mu$ g every 72 h for 2 weeks) as previously described [12]. LY294002 or vehicle were applied 5 h prior to each FA application. Mice were sacrificed and skin harvested for RNA isolation and histological/morphometric analysis 24 h after the last FA treatment.

### 2.18. Ear edema test

Mouse ears were pretreated with either vehicle or LY294002 (10 nmoles/ear) 5 h prior to treatment with contact irritant CO (20  $\mu$ L of 5% solution in acetone). FA (1  $\mu$ g/ear) was applied one hr prior to CO. Animals were sacrificed and ears harvested at the peak of inflammatory response, 9 h after CO application [8]. Ear swelling, a readout for inflammation, was measured by weighing 5 mm ear punches.

### 2.19. Morphometric analysis

Hematoxylin and eosin (H&E) staining was done in formalin-fixed, paraffin-embedded skin samples. The quantification of the epidermal and subcutaneous adipose tissue width, as a readout of skin atrophy, was performed as described [8]. The number of dermal cells was determined as described [12]. Proliferative index was calculated as a relative number of BrdU+ basal keratinocytes to the total number of basal keratinocytes. For all morphometric analyses, at least ten individual fields of view/slide in four individual skin samples (40 images/treatment group) were analyzed.

### 2.20. Statistical analysis

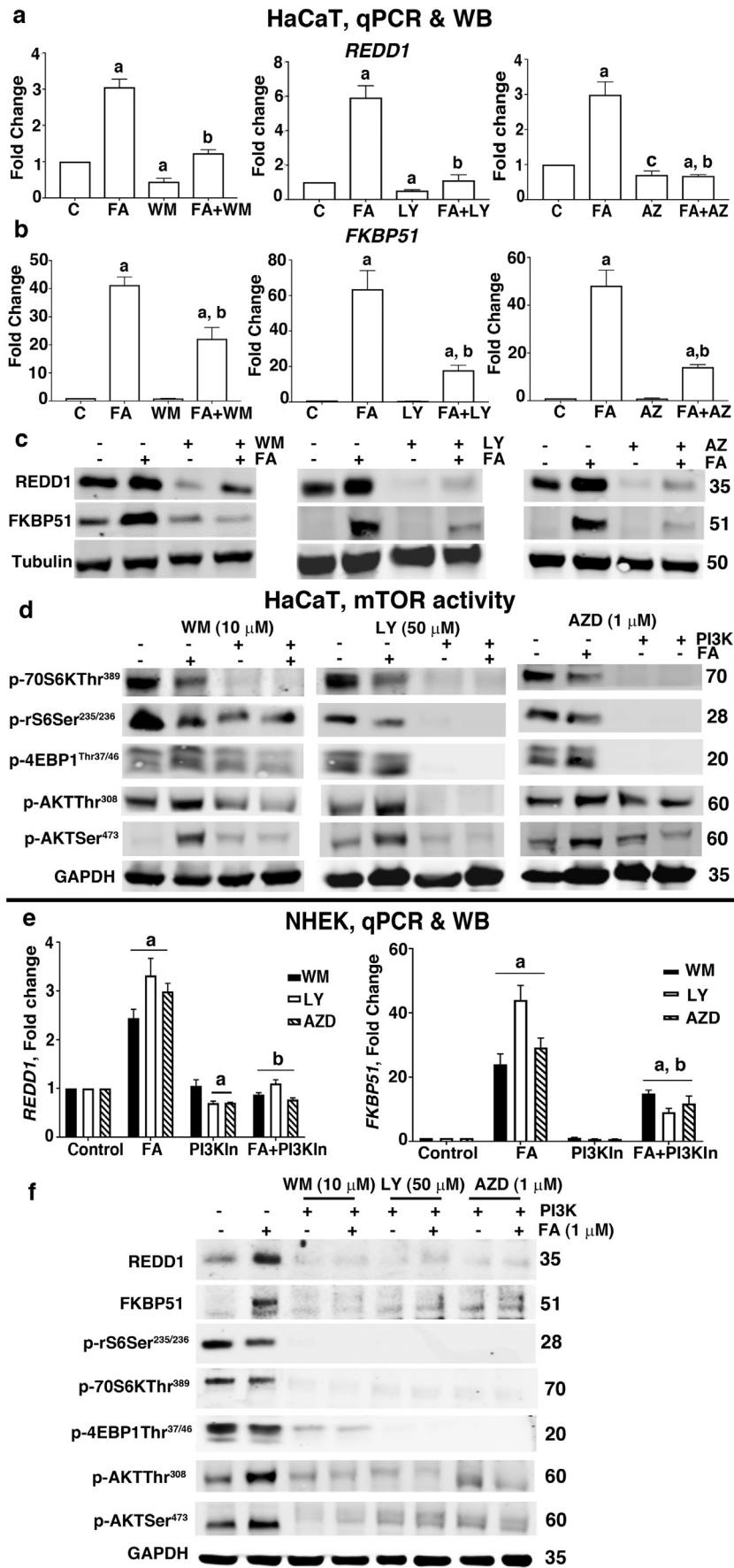
All experiments were conducted at least in duplicates. Mean and standard deviation were calculated using Microsoft Excel software. Statistical analyses of the data were performed by non-parametric unpaired two-tailed/sided Student's *t*-test using GraphPad Prism software (version 7.03). A P value < 0.05 was considered statistically significant.

## 3. Results

### 3.1. Bioinformatics search for small molecule REDD1 and FKBP51 inhibitors

To search for dual REDD1/FKBP51 inhibitors, we screened LINCS library (<http://lincsproject.org/LINCS/>) comprised of molecular signatures of ~20,000 FDA-approved and experimental drugs tested in a large array of human cells. We first scored compounds according to the number of LINCS experiments in which REDD1 expression was significantly inhibited (REDD1 was within top 100 down-regulated genes), and then selected those that also had negative effect on FKBP51 expression (Supplemental Table S1). Unexpectedly, we found that inhibitors of the PI3K/mTOR/Akt pathway represented the major drug class among the top 20 REDD1/FKBP51 inhibitors.

It is known that PI3K activation leads to the phosphorylation and activation of the protein kinase Akt, which in turn activates mTOR in both mTORC1 and mTORC2 complexes [28]. Thus, most of these putative



REDD1/FKBP51 inhibitors are known to affect to some degree all branches of PI3K/mTOR/Akt signaling. We selected several inhibitors with mixed profile from the Supplementary Table 1: classical experimental PI3K inhibitors WM and LY294002; PI3K/mTOR inhibitors Dactolisib/NVP-BEZ235 (NVP) and mTOR inhibitor AZD8055 that entered clinical trials as anti-cancer drugs [36,37]. In addition, we included in our studies a more selective Akt inhibitor MK-2206 (MK), also in clinical trials [38].

### 3.2. PI3K/mTOR/Akt inhibitors negatively impacted REDD1 and FKBP51 induction by glucocorticoid FA

We assessed the impact of selected PI3K/mTOR/Akt inhibitors on the expression of atrophogenes REDD1 and FKBP51 in immortalized human keratinocyte cell line HaCaT and primary human epidermal keratinocytes (NHEK). The concentration range of compounds (1–50  $\mu$ M) and the time of cells pre-treatment (6 h) in our experiments followed the experimental design of tests presented in LINCS database as well as the concentrations used in previous in vitro studies of these compounds [39–42].

To prove that the chosen experimental conditions indeed lead to the inhibition of PI3K/mTOR/Akt signaling, we assessed the effect of WM, LY294002 and AZD8055 on phosphorylation of mTOR downstream substrates 4E-BP1 (eukaryotic initiation factor 4E binding protein 1), p-70S6K kinase and its substrate rpS6 (ribosomal protein S6) and Akt phosphorylation at Thr308 and Ser473, the two major sites regulating Akt activity. As expected, we confirmed that under selected test conditions these compounds strongly inhibited PI3K/mTOR/Akt signaling in both keratinocyte models (Fig. 1d, f) with the exception of weaker effect of AZD8055 on Akt phosphorylation at Thr<sup>306</sup>. The effects on mTOR/Akt signaling were specific as the results of MTT assay clearly indicated that PI3K/mTOR/Akt inhibitors alone or in combination with glucocorticoid FA did not significantly affect keratinocyte viability during the experiments (Fig. S2).

We showed recently that GCs induced expression of REDD1 and FKBP51 in keratinocytes and in human skin [12,18]. In good correlation with these previous studies, REDD1 and FKBP51 expression at mRNA/protein levels was strongly increased in HaCaT and NHEK cells treated with FA (Fig. 1a–c, e, f; Fig. S1). All five PI3K/mTOR/Akt inhibitors under study powerfully blocked REDD1 and FKBP51 induction by FA at both mRNA and protein levels in HaCaT and NHEK keratinocytes (Fig. 1a–c, e, f; Fig. S1). The only exception was modest effect of NVP on REDD1 protein expression in HaCaT cells despite the significant inhibition of REDD1 mRNA induction by FA in those cells (Fig. 1a, c). In most cases PI3K/mTOR/Akt inhibitors (again with the exception of NVP) also significantly down-regulated basal REDD1 expression, especially visible on Western blots (Fig. 1c, f; Fig. S1c, f). However, their effect on the basal FKBP51 mRNA/protein levels was minimal most likely due to a low baseline FKBP51 expression (Figs. 1 and S1).

### 3.3. PI3K/mTOR/Akt inhibitors modified GR signaling and shifted it towards transrepression

REDD1 and FKBP51 are part of GR molecular signature in skin [12,18]. Thus, our results suggested that PI3K/mTOR/Akt inhibitors could modulate GR activity. To assess their potential to modify both GR signaling branches (transactivation/TA and transrepression/TR) we infected keratinocytes with lentiviruses expressing GRE-Luciferase and NF- $\kappa$ B-Luciferase reporters as inhibition of NF- $\kappa$ B is central to the

glucocorticoid anti-inflammatory activity and is usually used to monitor the effects on GR TR [6,43,44]. Pretreatment of HaCaT and NHEK keratinocytes with PI3K/mTOR/Akt inhibitors WM, LY294002; and AZD8055 blunted GR TA and exaggerated GR TR function evaluated by Luciferase assay (Fig. 2a, b).

Since LY294002 and AZD8055 alone significantly affected NF- $\kappa$ B-Luciferase activity in keratinocytes, it was interesting to assess their effect on NF- $\kappa$ B in more detail. For these experiments, HaCaT cells were activated by TNF- $\alpha$  ( $10^{-9}$  M  $\times$  30 min), which resulted in increased phosphorylation (at Ser32) and degradation of NF- $\kappa$ B inhibitor I $\kappa$ B $\alpha$ , followed by nuclear translocation of activated by phosphorylation (at Ser<sup>536</sup>) NF- $\kappa$ B protein p65/RelA (Fig. 2c). We found that pre-treatment of cells with both LY294002 and AZD8055 inhibited all major steps of NF- $\kappa$ B activation including phosphorylation/degradation of I $\kappa$ B $\alpha$  and p65/Rel phosphorylation/translocation to the nucleus (Fig. 2c). These results suggest that negative effect of PI3K/mTOR/Akt inhibitors on NF- $\kappa$ B signaling may contribute to GR TR when they are combined with glucocorticoid FA. Interestingly, even though WM strongly inhibited I $\kappa$ B $\alpha$  degradation and p65 nuclear import in HaCaT cells within 15 min after TNF- $\alpha$  addition (Fig. 2c), its effect on NF- $\kappa$ B-Luc, which was measured later, appeared to be modest (Fig. 2b).

Overall, Luciferase reporter assays revealed that the PI3K/mTOR/Akt inhibitors significantly modified GR signaling. To further corroborate this unexpected finding, we used Illumina Human HT-12 microarray to assess the global effect of one of the tested compounds, LY294002, on FA molecular signature in HaCaT keratinocytes (GEO submission GSE120991). Cells were treated with solvent (DMSO); FA only and LY294002 (pretreatment for 6 h) with FA. We incubated cells with FA for 24 h, a time point when both GR TA and TR are usually fully developed [45].

We identified 706 differentially expressed genes (DEG, P value <.01, FDR <.01) affected by FA with equal involvement of TA and TR branches of GR signaling: 374 genes were up-regulated, and 332 down-regulated. The top up- and down-regulated genes are presented in Supplemental Table S2.

In general, the FA molecular signature in human HaCaT keratinocytes reflected different facets of GR signaling, including known anti-inflammatory and metabolic effects, regulation of proliferation, differentiation, apoptosis, cell contacts, and ECM. In addition, we revealed novel aspects of GR crosstalk with major signaling pathways in skin such as Wnt, Notch, and TGF- $\alpha$  (via frizzled protein SFRP1, Notch effector HEY1, and multiple BMP regulators (Supplemental Table S2). Importantly, there was a significant similarity between molecular signatures of glucocorticoids in HaCaT human keratinocytes and human skin [2] (GEO submission GSE120783) with >65 identical DEGs (Supplemental Table S3), suggesting that HaCaT cells are a reliable in vitro model to study GR signaling in skin. The group of identical DEGs includes genes that play causative role in skin atrophy FKBP51 and DDIT4/REDD1; metabolism regulators PLIN2, PNLI3, GLUL and HSD11B2 that converts cortisol into non-active cortisone; regulators of ion channels BEST2 and SCNN1G; regulators of apoptosis BIRC3/IAP3 and SGK1 to name a few.

In order to look at systemic effects of FA on transcriptome in keratinocytes, we performed gene set enrichment (GSE) analysis using GO and Hallmark gene sets from Molecular Signatures Database (MSigDB) (Supplemental Table S4). Consistent with the known glucocorticoid effects, highly enriched processes were inflammatory/immune pathways including TNF $\alpha$ , NF- $\kappa$ B, IL2/STAT5 signaling; stress response to UV and hypoxia; sodium and other metal transport [2,46,47]. In

**Fig. 1.** PI3K/mTOR/Akt inhibitors prevent activation of key atrophogenes, REDD1 and FKBP51 in HaCaT cells and NHEK primary human keratinocytes. HaCaT cells (a–d) and NHEK cells (e–f) were pretreated with solvent (Control), WM (10  $\mu$ M), LY294002 (50  $\mu$ M) and AZD8055 (1  $\mu$ M) for 6 h and treated with either solvent or glucocorticoid FA (1  $\mu$ M) for 24 h. (a, b, e) Q-PCR analysis of REDD1 and FKBP51 mRNA expression in HaCaT (a, b) and NHEK (e) cells. The Q-PCR results were normalized to the expression of housekeeping gene RPL27, and presented as fold change compared to control. The mean  $\pm$  SD was calculated for three individual RNA samples/condition. Statistically significant differences as compared to: a-control (DMSO) (P <.001); b-FA (P <.001); c-control (DMSO) (p <.5) (two-tailed unpaired t-test). (c, d, f) Western blot analysis of REDD1 and FKBP51 protein levels, phosphorylation of mTOR downstream substrates and Akt phosphorylation at Thr308 and Ser473 in HaCaT (c, d) and NHEK (f) keratinocytes. Tubulin and GAPDH were used as the loading controls.

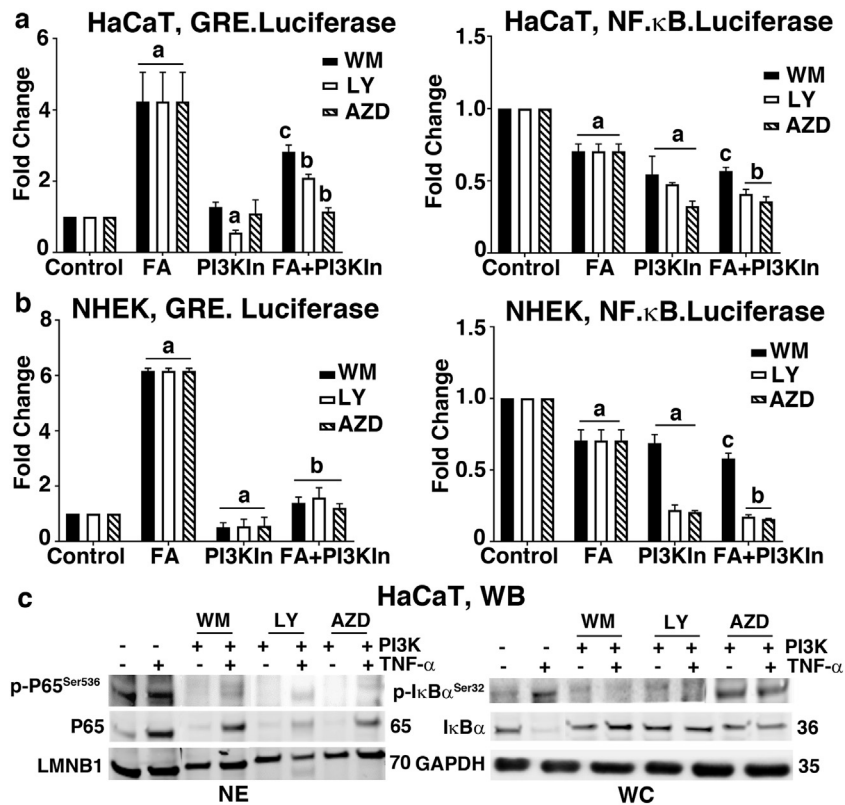


**Fig. 2.** PI3K/mTOR/Akt inhibitors reduce GR transactivation, block NF-κB and enhance GR transrepression. (a, b) Luciferase assay. HaCaT and NHEK cells stably expressing GRE.Luciferase and NF-κB.Luciferase were pretreated with WM (10 μM), LY294002 (50 μM) and AZD8055 (1 μM) for 6 h and treated with either solvent (Control) or FA (1 μM) for 24 h. Luciferase expression is presented as mean ± SD for 3 individual wells/point. Statistically significant differences as compared to: a-control ( $P < .001$ ); b-FA ( $P < .001$ ); c-FA ( $p < .05$ ) (two-tailed unpaired  $t$ -test). (c) Western blot analysis of NF-κB activation. HaCaT cells treated with solvent or indicated inhibitor for 24 h were stimulated with TNF-α (50 ng/mL x 15 min). The levels of phosphorylated and non-phosphorylated p65 and IκBα proteins were analyzed by Western blotting ( $n = 3$ ). GAPDH and lamin B served as loading controls for cytoplasmic and nuclear proteins respectively. NE, nuclear extract; WC, whole cell extract.

addition, significant part of top gene sets included genes involved in development; EMT (epithelial–mesenchymal transition) that reflected known negative effect of glucocorticoids on cell-cell adhesion [47]; estrogen response and cross-talk with K-ras signaling.

In the presence of LY294002, most of FA-induced DEGs remained differentially expressed with preserved direction of changes: 59% of DEGs up-regulated by FA and of 74% of DEGs down-regulated by FA remained up-regulated and down-regulated in the presence of LY294002. However, we observed that LY294002 very significantly exaggerated GR TR (FA + LY vs. FA,  $t$ -test: 3.64;  $p$  value:  $4e-4$ ; 2-sample, paired  $t$ -test, Fig. 3a). We also observed a trend to the inhibition of GR TA by LY294002 (FA + LY vs. FA,  $t$ -test: 1.36;  $p$  value: 0.17) (Fig. 3a). The top DEGs with blunted TA or enhanced TR are presented in the Supplemental Table S5. We validated microarray results using Q-PCR analysis by selecting a dozen of genes from both up-regulated and down-regulated categories (Fig. 3b, Supplemental Table S6), and confirmed that PI3K/mTOR/Akt inhibitor LY294002 blunted GR TA, and exaggerated GR TR.

The rest of the FA-induced DEGs either did not change significantly compared to control or became DEGs with reversed (compared to FA only) changes in the presence of LY294002. This latter relatively small group of 13 DEGs included genes involved in apoptosis, proliferation, epithelial differentiation, and metabolism of cholesterol, retinoic acid and glucocorticoids (Supplemental Table S7).

#### 3.4. PI3K/mTOR/Akt inhibitors reduced GR phosphorylation, nuclear translocation and binding to REDD1 and FKBP51 promoters

To identify the molecular mechanisms underlying GR functional changes induced by PI3K/mTOR/Akt inhibitors, we assessed how these compounds affect important GR activation steps, such as phosphorylation,

nuclear translocation and loading on glucocorticoid response elements (GREs) in REDD1 and FKBP51 promoters.

In FA-stimulated HaCaT cells, GR phosphorylation and nuclear translocation occurred in 10 min, and GR remained in the nucleus for at least 12 h (Fig. 4a, b). Pretreatment of cells with WM and LY294002 either delayed or decreased GR phosphorylation and nuclear import (Fig. 4a, b). They also accelerated GR nuclear export: the amount of nuclear GR returned to control levels in ~4 h in cells pretreated with PI3K/mTOR/Akt inhibitors (Fig. 4b). The decreased amount of GR in the nucleus in cells treated with FA + LY294002 possibly reflects the increased GR nuclear-cytoplasm shuttling. The immunofluorescence data substantiated our Western blot results (Supplemental Fig. S3), even though with this method we revealed a more significant amount of GR in the nucleus of control cells.

Next, we analyzed whether WM and LY294002 affected GR loading on known GRE sites in human REDD1 and FKBP51 promoters. Interestingly, both compounds prevented GR binding to REDD1 and FKBP51 promoters (Fig. 4c, d) thereby inhibiting REDD1 and FKBP51 expression activation by FA (Fig. 1a). Moreover, WM and LY294002 reduced GR basal occupancy at these promoter regions (compare to enrichment obtained in cells treated with DMSO, Fig. 4c, d) which probably contributes to the reduced expression of these GR-target genes in HaCaT cells treated with PI3K/mTOR/Akt inhibitors alone versus control, especially noticeable for REDD1 (Fig. 1a, b).

#### 3.5. LY294002 spared mouse skin from FA-induced atrophy but did not interfere with FA's anti-inflammatory effects

We have chosen LY294002 to assess in vivo effects of PI3K/mTOR/Akt inhibitors, as it was previously used in experiments with topical

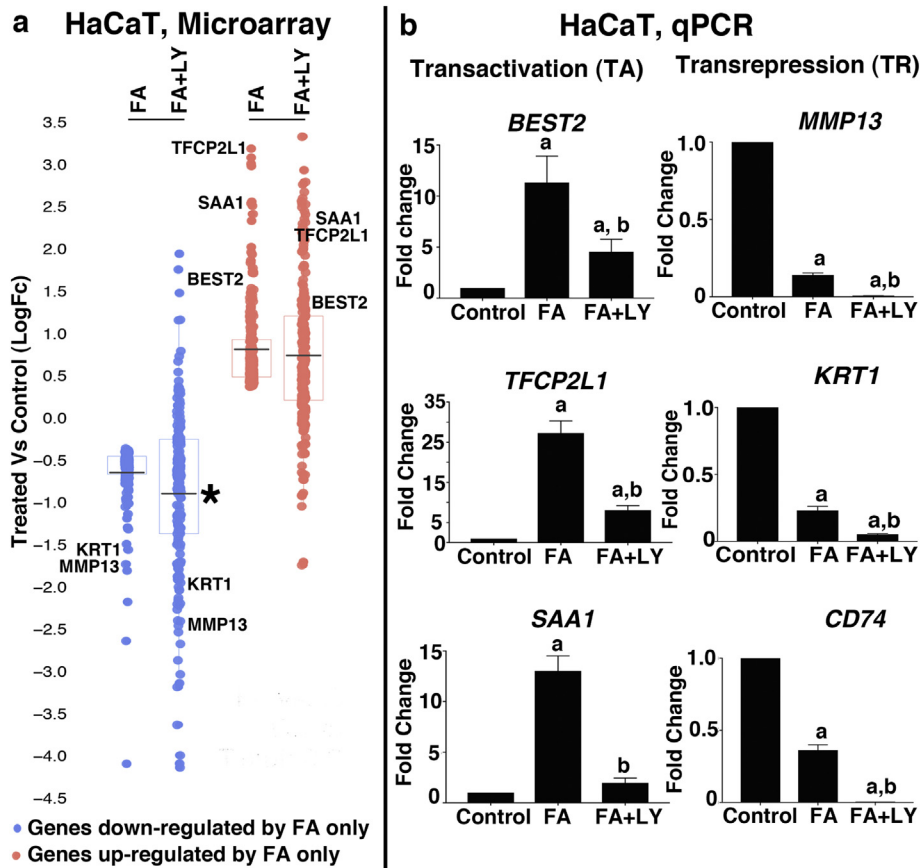


**Fig. 3.** Illumina array analysis of LY294002 global effect on glucocorticoid-induced differential gene expression. (a) HaCaT cells were treated with vehicle (Control), FA (1  $\mu$ M, 24 h) or FA after pretreatment with LY294002 (50  $\mu$ M, 6 h). Total RNA was extracted from cells in two independent experiments and used for analysis of gene expression by HT-12 Illumina microarray. X-axis, Experimental groups. Y-axis, Box plot of top 150 most up- and down-regulated DEGs (based on log<sub>2</sub> fold changes, logFC). Box plot encompasses 1st and 3rd quartiles of logFC. Left set: genes down-regulated by FA only. Right set: genes up-regulated by FA only. Horizontal black lines indicate mean. Genes validated via Q-PCR are presented. \* Statistically significant changes for down-regulated genes (in blue) FA + LY vs. FA, T-statistic: -3.64; p value: 4e-4 (2-sample, paired t-test). For up-regulated genes (in red) FA + LY vs. FA, T-statistic: -1.36; p value: 0.17. (b) Array validation by Q-PCR. The Q-PCR results were normalized to the housekeeping gene RPL27, and presented as fold change compared to control. The mean  $\pm$  SD was calculated for three individual RNA samples/condition. Statistically significant differences as compared to: a-control (P < .001); b-FA (P < .001 (two-tailed unpaired t-test)).

applications to the skin [48,49]. F1 C57Bl x 129 mice were topically treated with FA (1  $\mu$ g/animal) in the presence or absence of LY294002 (10 nmoles/animal). We used special formulation: 30% PEG3350, 4% DMSO, 5% Tween 20 in PBS for the optimal transepidermal LY294002 delivery.

As expected, acute treatment with FA significantly induced expression of REDD1 and FKBP51 mRNAs, and pre-treatment of skin with LY294002 blocked this FA effect (Fig. 5a).

The steroid-induced skin atrophy has been well described morphologically; it involves all skin compartments and results in overall skin thinning, reduction in size and number of keratinocytes, inhibition of dermal fibroblast proliferation and collagen synthesis, atrophy of dermal adipose and epidermal appendages. To test whether LY294002 could prevent development of FA-induced skin atrophy, we chronically treated mice with FA  $\pm$  LY294002 every 72 h for 2 weeks. In agreement with our published results [12], chronic treatment with FA led to severe cutaneous atrophy: epidermal thickness was reduced by ~50%, dermal cellularity was decreased by 78%, dermal adipose tissue was reduced by ~90% (Fig. 5c–f). Remarkably, LY294002 significantly protected skin from these hypoplastic effects of FA: LY + FA-treated skin displayed only 22% and 50% reduction in epidermal and dermal adipose thickness accordingly (Fig. 5c–e). LY294002 also protected dermis as assessed by the decreased effects of FA on dermal cellularity (Fig. 5f) and on expression of Col3A1 (Fig. 5g) considered a major marker for inhibitory effect of GCs on collagen synthesis [50,51].

In our next experiments we assessed proliferation in epidermis by incorporation of 5-bromo-2'-deoxyuridine (BrdU) into basal keratinocytes. In mouse skin treated with FA for 24 h, the BrdU-labeling index dropped to  $1.2 \pm 1.4\%$  from  $4.9 \pm 1.4\%$  in control. However, in skin treated with LY + FA, BrdU labeling index remained similar to control:  $4.7 \pm 3.4\%$  (Fig. 5b).

To test whether LY294002 affects anti-inflammatory effect of glucocorticoids, we used standard ear edema test. Mouse ears were treated with irritant croton oil (CO) in the presence or absence of LY294002 (10 nmoles/ear) and FA (1  $\mu$ g/ear), and ear edema at 9 h after CO application was used as a readout for inflammation, as published previously [12]. CO induced inflammation and ear swelling, and FA completely blocked it, in line with previously published results [12]. The pre-treatment with LY294002 did not affect either CO-induced inflammation or anti-inflammatory effect of FA (Fig. 5h).

#### 4. Discussion

The adverse effects associated with chronic glucocorticoid treatment motivated development of novel GR ligands. Dozens of selective GR activators and modulators (SEGRAM) have been synthesized and tested by industry and academia, however, the success was rather limited [15]. In the current work, we present data demonstrating the advantages of alternative approach to safer GR-targeted therapies via combination of glucocorticoids with anti-atrophogenic tissue protectors.

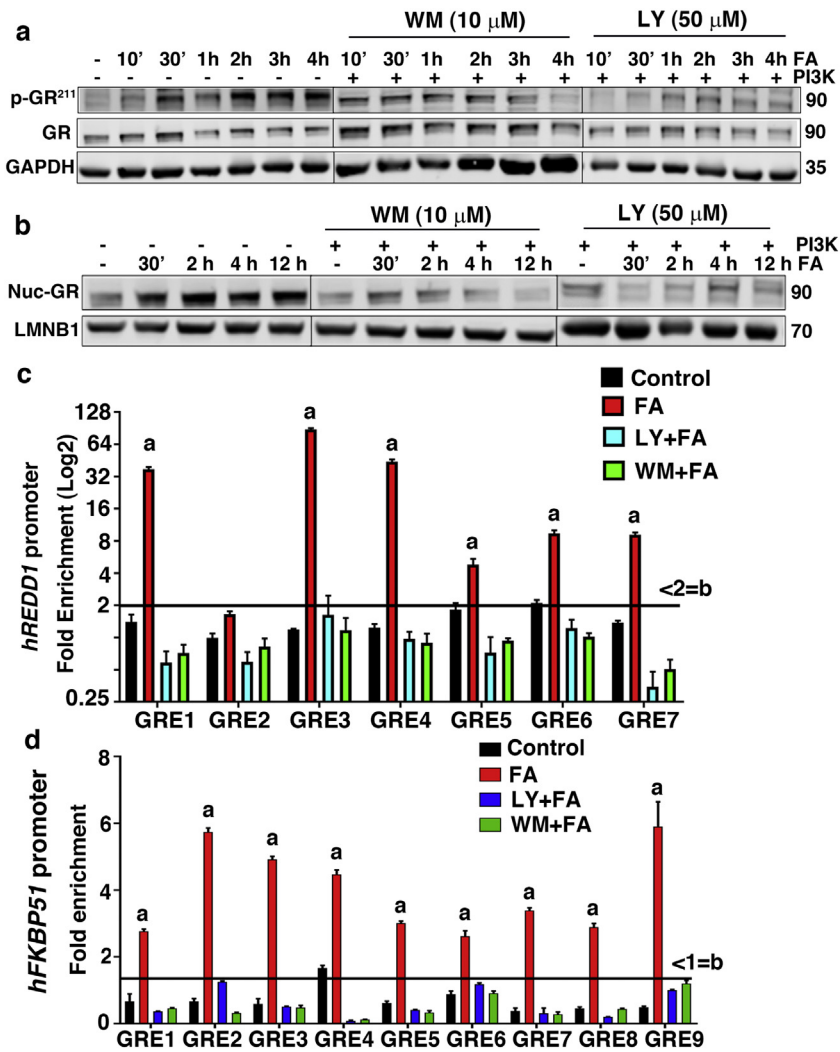


**Fig. 4.** PI3K/mTOR/Akt inhibitors negatively affect GR phosphorylation, nuclear translocation and binding to GREs in REDD1 and FKBP51 promoters. (a) Western blot analysis of total and phosphorylated GR in HaCaT cells. Cells were pretreated with solvent, WM (10  $\mu$ M) or LY294002 (50  $\mu$ M) for 6 h followed by FA (1  $\mu$ M) for 24 h. Whole cell proteins were used for Western blotting. GAPDH served as the loading control. (b) Western blot analysis of the nuclear extracts extracted from HaCaT cells pretreated with WM and LY294002 for 6 h at the doses indicated above and treated with FA (1  $\mu$ M) for indicated time. Nuclear protein lamin B was used as loading control. (c, d) GR loading on GREs in REDD1 promoter (C), and in FKBP51 promoter (D) was assessed by ChIP in HaCaT cells treated (3 independent experiments) either with solvent (control), FA (1  $\mu$ M  $\times$  24 h) or pretreated for 6 h with either WM (10  $\mu$ M) or LY294002 (50  $\mu$ M) followed by addition of FA (1  $\mu$ M  $\times$  24 h). Statistically significant difference compared to: a-control ( $P < .001$ ); b-FA ( $P < .001$ ) (two-tailed unpaired t-test). Data are mean  $\pm$  SD.

We searched for REDD1/FKBP51 pharmacological inhibitors by computational screening of NIH LINCS database (<http://lincsproject.org/LINCS/>) generated as a catalog of changes in gene expression and other cellular processes induced in a large variety of cells exposed to >20,000 small molecule drugs. Almost 50% of the top repurposing candidates targeting REDD1 and FKBP51 expression, appeared to belong to the class of PI3K/mTOR/Akt inhibitors. This finding is in line with our previous search for REDD1 inhibitors using much smaller CMAP library consisting of molecular signatures of ~1300 FDA-approved drugs (<https://www.broadinstitute.org/cmap/>), which revealed mTOR inhibitor Rapamycin as the top repurposing candidate [30]. These predictions were completely unexpected as PI3K/mTOR/Akt inhibitors have been developed as anti-cancer drugs inhibiting cell proliferation. In this context, it is interesting to mention that cutaneous side effects are typical for many classes of anti-cancer drugs including mTOR inhibitors. However, anti-cancer drugs usually induce skin inflammation but not skin atrophy [16,52].

We experimentally validated the capability of PI3K/mTOR/Akt inhibitors to suppress REDD1 and FKBP51 expression at mRNA and protein levels (Fig. 1, Supplemental Fig. S1) in vivo in mice, and in vitro in monolayer human keratinocyte models. In the future, it would be

important to assess the effect of these anti-REDD1/FKBP51 drugs in organotypic raft cultures that are more physiologically relevant to human skin.

It was shown previously that mTOR regulates proteasomal degradation of its genetic inhibitor REDD1 [53] and work presented here further corroborated mTOR-controlled REDD1 regulation. Even though the post-translational modifications of FKBP51 including phosphorylation, SUMOylation and ubiquitination were reported [22], the existence of similar FKBP51/mTOR/AKT feedback loop in the regulation of FKBP51 protein turnover and stability is presently not known.

Surprisingly, we found that inhibitors from this pharmacological class also strongly modified GR activity shifting it towards TR signaling branch. This occurred via global enhancement of TR which in part reflects the cooperative repression of NF- $\kappa$ B by glucocorticoid (FA) and PI3K/mTOR/Akt inhibitors that suppressed I $\kappa$ B $\alpha$  degradation and nuclear import of p65 (Fig. 2c). These stages in NF- $\kappa$ B activation are usually not affected by glucocorticoids [54]. We also observed a trend for the GR TA global decrease confirmed by GRE.Luciferase assay and reduced activation of a large cohort of endogenous genes (Fig. 3, Supplemental Tables S2, S5 and S6). Importantly, we observed the same GR signaling shift to TR in cells pretreated with Rapamycin [30]. Overall, our results

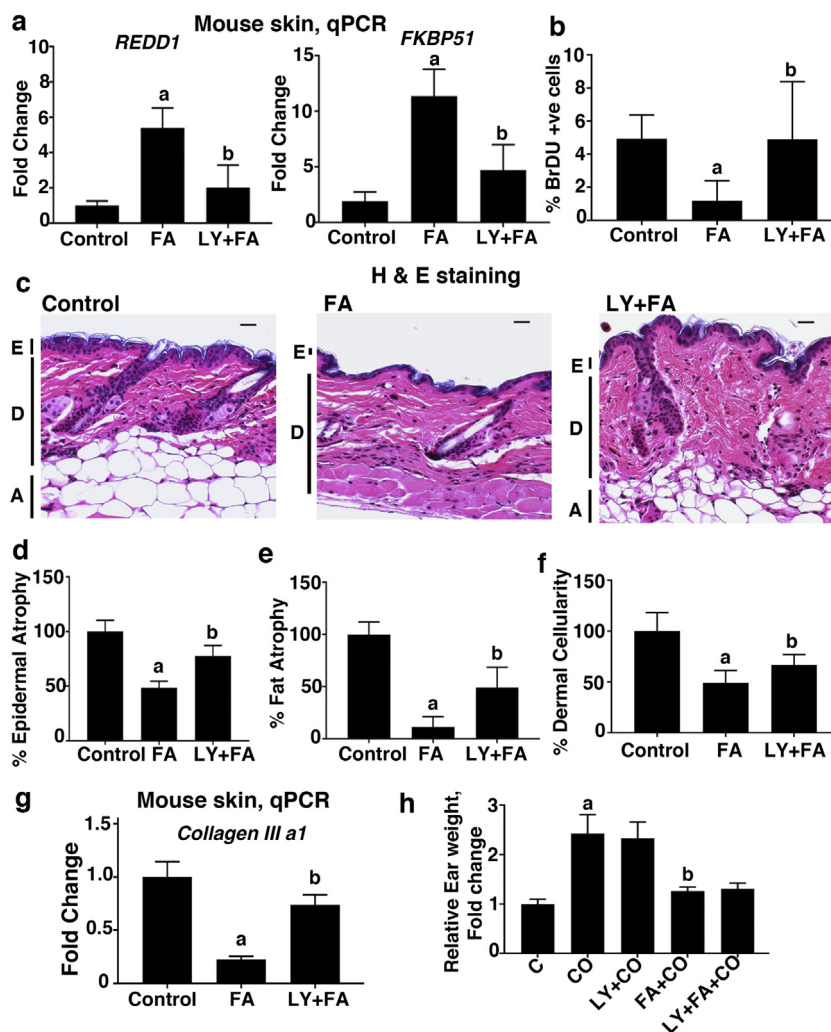


**Fig. 5.** LY294002 protects skin against FA-induced atrophy but does not affect FA anti-inflammatory activity. Animals ( $n = 4/\text{group}$ ) were treated with solvent or FA ( $1 \mu\text{g}/\text{animal}$ ) with or without LY294002 pre-treatment ( $10 \text{ nmoles}/\text{animal} \times 5 \text{ h}$ , applied in skin formulation as described in materials and methods). (a) Q-PCR analysis of REDD1 and FKBP51 expression in epidermis 8 h after FA application. RPL27 gene was used as a loading control. Data are presented as mean  $\pm$  SD fold change of mRNA expression as compared to control. Statistically significant difference compared to: a-control ( $P < .001$ ); b- FA ( $P < .05$ ) (two-tailed unpaired t-test). (b) Quantification of proliferation in skin. Animals were treated as above, injected intraperitoneally with BrdU (as in Materials and Methods), and skin was harvested 24 h after FA application. BrdU-positive cells were identified by immunostaining. Results are percent of BrdU+ basal keratinocytes presented as mean  $\pm$  SD,  $n = 4$ . Statistically significant difference compared to: a-control ( $P < .001$ ); b- FA ( $P < .005$ ) (two-tailed unpaired t-test) (c, d, e). Skin atrophy tests. Animals were treated as described, every 72 h for 2 weeks, and sacrificed 24 h after the last FA treatment. (c) H&E staining. (d,e) Morphometric analysis of epidermal and dermal adipose atrophy, data are expressed as percent to corresponding control and presented as mean  $\pm$  SD,  $n = 4$ . Statistically significant difference compared to: a-control ( $P < .001$ ); b- FA ( $P < .001$ ) (two-tailed unpaired t-test). (f) Morphometric analysis of dermal cellularity, data are expressed as percent to corresponding control and presented as mean  $\pm$  SD,  $n = 4$ . Statistically significant difference compared to: a-control ( $P < .01$ ); b- FA ( $P < .05$ ) (two-tailed unpaired t-test). (g) Q-PCR analysis of collagen type III a1 (*col3a1*) expression in chronically treated skins. RPL27 gene was used as a loading control. Data are presented as mean  $\pm$  SD fold change of mRNA expression as compared to control. Statistically significant difference compared to: a-control ( $P < .01$ ); b- FA ( $P < .05$ ) (two-tailed unpaired t-test). (h) Croton-oil induced ear edema after pre-treatment with FA; LY294002 or FA + LY. The weight of 5 mm ear punch (inflammation readout) is presented as fold change compared to control. Data are mean  $\pm$  SD for 6 ear punches/condition. Statistically significant difference CO versus control (a- $P < .001$ ); CO versus CO + FA (b-  $P < .004$ ) (two-tailed unpaired t-test). Note: LY did not affect ear either swelling or anti-inflammatory effect of FA.

suggest that in the presence of PI3K/mTOR/Akt inhibitors glucocorticoids behave as long awaited SEGRAMs shifting GR activity towards therapeutically significant TR.

GR activity depends on many factors including GR phosphorylation and efficient nuclear import, presence of co-regulatory proteins [8,9,11,13,54,55]. GR is phosphorylated on multiple serine and threonine residues at its N-terminus by mitogen-activated protein kinases (MAPKs), cyclin-dependent kinases (CDKs), casein kinase II and glycogen synthase kinase-3 $\beta$  (GSK-3 $\beta$ ), and GR phosphorylation status defines its nuclear import and functions [56–58]. Several tested PI3K/mTOR/Akt inhibitors: LY294002, WM (as presented here) and Rapamycin [30], but not AZD8055 (not shown), inhibited GR phosphorylation at activating Ser211 and decreased GR nuclear import. It is possible that this group of inhibitors affected GR kinases as mTOR and Akt crosstalk with signaling pathways involving p38, GSK-3beta is known

[59,60]. The possible alternative mechanisms of GR signaling modification by REDD1/FKBP51 inhibitors that did not affect GR phosphorylation (like AZD8055), are currently under study.

Besides discussed above mechanisms of GR modulation, both GR target genes in the focus of this study, REDD1 and FKBP51, play an important role in control of the GR signaling, and this adds the further level of complexity to the understanding of GR- PI3K/mTOR/Akt cross-talk. We recently found that the lack of REDD1 hampers GR TA [12]. On the other hand; FKBP51 is a known GR chaperone, and negative regulator of its nuclear import and transcriptional activity [22]. Interestingly, we did not observe changes in GR intracellular localization and function in human keratinocytes and in mouse skin after FKBP51 knockout [18] suggesting that FKBP51 effects on GR function are cell type-specific.

Many PI3K/mTOR/Akt inhibitors are currently in clinic/clinical trials as anti-cancer drugs and immunomodulators (Rapamycin), however,

their use in dermatology has been very limited. Our *in vivo* results showed that LY294002 (Fig. 5) and Rapamycin [30] were able to prevent FA-induced skin atrophy, but did not interfere with FA's anti-inflammatory effects. Thus, our studies provide a proof of principle for using compounds from this pharmacological class to prevent atrophic effects induced by chronically applied glucocorticoids in skin. In addition to skin atrophy, chronic treatment with GCs results in other adverse effects including delayed wound healing, pigment alteration, increased risk of skin infections [16,61–63]. It will be important to test whether PI3K/mTOR/Akt inhibitors can ameliorate these cutaneous side effects of GCs. The corticosteroids induce atrophy in many organs besides skin [7,18,64,65]. We previously revealed a strong similarity between GR molecular signatures in muscle, epidermis, dermal adipose undergoing steroid-induced atrophic changes [12,30], suggesting that the same approach to GR-targeted therapies using glucocorticoids in combination with tissue protectors is applicable for the treatment of patients with non-dermatological inflammatory and autoimmune diseases such as inflammatory bowel disease, rheumatoid arthritis, and asthma.

### Funding sources

Work is supported by R01GM112945, R01AI125366 (to IB and JTD), HESI-THRIVE grant (to IB).

### Declaration of interests

None exist.

### Author contributions

JTD, IB, SA-Conceived the study plan, analyzed the data and wrote the manuscript; SA-performed all *in vitro* experiments; SM-performed, analyzed and wrote the *in vivo* mouse experiment; IB, BR-analyzed and compiled the microarray data.

### Acknowledgements

We acknowledge University of Chicago Genomics Facility where Illumina microarray was performed, and Northwestern University SDRC (5 P30 AR057216) morphology and phenotyping, skin tissue engineering, and DNA/RNA delivery Cores for their technical support.

### Appendix A. Supplementary data

Supplementary data to this article can be found online at <https://doi.org/10.1016/j.ebiom.2019.01.055>.

### References

- Chebotaev D, Yemelyanov A, Budunova I. The mechanisms of tumor suppressor effects of glucocorticoid receptor in skin. *Mol Carcinog* 2007;46(8):732–40.
- Sarkar MK, Kaplan N, Tsoi LC, et al. Endogenous glucocorticoid deficiency in psoriasis promotes inflammation and abnormal differentiation. *J Invest Dermatol* 2017;137(7):1474–83.
- Slominski AT, Manna PR, Tuckey RC. On the role of skin in the regulation of local and systemic steroidogenic activities. *Steroids* 2015;103:72–88.
- Slominski AT, Zbytek B, Nikolakis G, et al. Steroidogenesis in the skin: implications for local immune functions. *J Steroid Biochem Mol Biol* 2013;137:107–23.
- Slominski A, Zjawiony J, Wortsman J, et al. A novel pathway for sequential transformation of 7-dehydrocholesterol and expression of the P450scc system in mammalian skin. *Eur J Biochem* 2004;271:4178–88.
- Slominski AT, Li W, Kim TK, Semak I, Wang J, Zjawiony JK, et al. Novel activities of CYP11A1 and their potential physiological significance. *J Steroid Biochem Mol Biol* 2015;151:25–37.
- Stern RS. The pattern of topical corticosteroid prescribing in the United States, 1989–1991. *J Am Acad Dermatol* 1996;35(2 Pt 1):183–6.
- Lesovaya E, Yemelyanov A, Swart AC, Swart P, Haegeman G, Budunova I. Discovery of compound A-a selective activator of the glucocorticoid receptor with anti-inflammatory and anti-cancer activity. *Oncotarget* 2015;6(31):30730–44.
- De Bosscher K, Haegeman G, Elewaut D. Targeting inflammation using selective glucocorticoid receptor modulators. *Curr Opin Pharmacol* 2010;10(4):497–504.
- Vandevyver S, Dejager L, Libert C. On the trail of the glucocorticoid receptor: into the nucleus and back. *Traffic* 2012;13(3):364–74.
- Ramamoorthy S, Cidlowski JA. Ligand-induced repression of the glucocorticoid receptor gene is mediated by an NCoR1 repression complex formed by long-range chromatin interactions with intragenic glucocorticoid response elements. *Mol Cell Biol* 2013;33(9):1711–22.
- Baida G, Bhalla P, Kirisanov K, Lesovaya E, Yakubovskaya M, Yuen K, et al. REDD1 functions at the crossroads between the therapeutic and adverse effects of topical glucocorticoids. *EMBO Mol Med* 2015;7(1):42–58.
- Ratman D, Vanden Berghe W, Dejager L, Libert C, Tavernier J, Beck IM, et al. How glucocorticoid receptors modulate the activity of other transcription factors: a scope beyond tethering. *Mol Cell Endocrinol* 2013;380(1–2):41–54.
- Cohen DM, Steger DJ. Nuclear receptor function through genomics: lessons from the glucocorticoid receptor. *Trends Endocrin Met* 2017;28(7):531–40.
- De Bosscher K, Beck IM, Ratman D, Berghe WV, Libert C. Activation of the glucocorticoid receptor in acute inflammation: the SEDIGRAM concept. *Trends Pharmacol Sci* 2016;37(1):4–16.
- Schoepe S, Schacke H, May E, Asadullah K. Glucocorticoid therapy-induced skin atrophy. *Exp Dermatol* 2006;15(6):406–20.
- Woodbury R, Kligman AM. The hairless mouse model for assaying the atrophogenicity of topical corticosteroids. *Acta Derm Venereol* 1992;72(6):403–6.
- Baida G, Bhalla P, Yemelyanov A, et al. Deletion of the glucocorticoid receptor chaperone FKBP51 prevents glucocorticoid-induced skin atrophy. *Oncotarget* 2018;9:34772–83.
- Shimizu N, Yoshikawa N, Ito N, et al. Crosstalk between glucocorticoid receptor and nutritional sensor mTOR in skeletal muscle. *Cell Metab* 2011;13(2):170–82.
- Shoshani T, Faerman A, Mett I, et al. Identification of a novel hypoxia-inducible factor 1-responsive gene, RTP801, involved in apoptosis. *Mol Cell Biol* 2002;22(7):2283–93.
- Ellisen LW. Growth control under stress: mTOR regulation through the REDD1-TSC pathway. *Cell Cycle* 2005;4(11):1500–2.
- Fries GR, Gassen NC, Rein T. The FKBP51 glucocorticoid receptor Co-chaperone: regulation, function, and implications in health and disease. *Int J Mol Sci* 2017;18(12):2614–44.
- Storer CL, Dickey CA, Galigniana MD, Rein T, Cox MB. FKBP51 and FKBP52 in signaling and disease. *Trends Endocrin Met* 2011;22(12):481–90.
- Manning BD, Cantley LC. AKT/PKB signaling: navigating downstream. *Cell* 2007;129(7):1261–74.
- Yung HW, Charnock-Jones DS, Burton GJ. Regulation of AKT phosphorylation at Ser473 and Thr308 by endoplasmic reticulum stress modulates substrate specificity in a severity dependent manner. *PLoS One* 2011;6(3):e17894.
- Alessi DR, Andjelkovic M, Caudwell B, Cron P, Morrice N, Cohen P, et al. Mechanism of activation of protein kinase B by insulin and IGF-1. *EMBO J* 1996;15(23):6541–51.
- Marz AM, Fabian AK, Kozary C, Bracher A, Hausch F. Large FK506-binding proteins shape the pharmacology of rapamycin. *Mol Cell Biol* 2013;33(7):1357–67.
- Dennis MD, Coleman CS, Berg A, Jefferson LS, Kimball SR. REDD1 enhances protein phosphatase 2A-mediated dephosphorylation of Akt to repress mTORC1 signaling. *Sci Signal* 2014;7(335):ra68.
- DeYoung MP, Horak P, Sofer A, Sgroi D, Ellisen LW. Hypoxia regulates TSC1/2-mTOR signaling and tumor suppression through REDD1-mediated 14-3-3 shuttling. *Genes Dev* 2008;22(2):239–51.
- Lesovaya E, Agarwal S, Readhead B, Vinokour E, Baida G, Bhalla P, et al. Rapamycin modulates glucocorticoid receptor function, blocks atrophogenic REDD1, and protects skin from steroid atrophy. *J Invest Dermatol* 2018;138(9):1935–44.
- Yevshin I, Sharipov R, Valeev T, Kel A, Kolpakov F. GTRD: a database of transcription factor binding sites identified by ChIP-seq experiments. *Nucleic Acids Res* 2017;45(D1):D61–7.
- Smyth GK, Limma: Linear Models for Microarray Data. In: Gentleman R, Carey VJ, Huber W, Irizarry RA, Dudoit S, editors. *Bioinformatics and Computational Biology Solutions Using R and Bioconductor*. Statistics for Biology and Health. New York, NY: Springer; 2005.
- Benjamini Yoav, Hochberg Yosef. Controlling the false discovery rate: a practical and powerful approach to multiple testing. *J R Stat Soc Series B Stat Methodol* 1995;57(1):289–300.
- Wickham H. *ggplot2: Elegant Graphics for Data Analysis*. New York: Springer-Verlag; 2009.
- Slominski A, Paus R. Melanogenesis is coupled to murine anagen: toward new concepts for the role of melanocytes and the regulation of melanogenesis in hair growth. *J Invest Dermatol* 1993;101(1):90S–7S.
- Naing A, Aghajanian C, Raymond E, et al. Safety, tolerability, pharmacokinetics and pharmacodynamics of AZD8055 in advanced solid tumours and lymphoma. *Br J Cancer* 2012;107(7):1093–9.
- Mukherjee B, Tomimatsu N, Amancherla K, Camacho CV, Pichamoorthy N, Burma S. The dual PI3K/mTOR inhibitor NVP-BEZ235 is a potent inhibitor of ATM- and DNA-PKCs-mediated DNA damage responses. *Neoplasia* 2012;14(1):34–43.
- Narayan RS, Fedrigo CA, Brands E, et al. The allosteric AKT inhibitor MK2206 shows a synergistic interaction with chemotherapy and radiotherapy in glioblastoma spheroid cultures. *BMC Cancer* 2017;17(1):204.
- Zhou BR, Huang QH, Xu Y, Wu D, Yin ZQ, Luo D. Dihydrotestosterone induces SREBP-1 expression and lipogenesis through the phosphoinositide 3-kinase/Akt pathway in HaCaT cells. *Lipids Health Dis* 2012;11:156.
- Nam HJ, Park YY, Yoon G, Cho H, Lee JH. Co-treatment with hepatocyte growth factor and TGF-beta1 enhances migration of HaCaT cells through NADPH oxidase-dependent ROS generation. *Exp Mol Med* 2010;42(4):270–9.

- [41] Bridgeman BB, Wang P, Ye B, Pelling JC, Volpert OV, Tong X. Inhibition of mTOR by apigenin in UVB-irradiated keratinocytes: a new implication of skin cancer prevention. *Cell Signal* 2016;28(5):460–8.
- [42] Hatzold J, Beleggia F, Herzig H, et al. Tumor suppression in basal keratinocytes via dual non-cell-autonomous functions of a Na,K-ATPase beta subunit. *Elife* 2016;5:e14277–306.
- [43] Schacke H, Hennekes H, Schottelius A, et al. SEGRAs: a novel class of anti-inflammatory compounds. *Ernst Schering Res Found Work* 2002;40:357–71.
- [44] Schacke H, Schottelius A, Docke WD, et al. Dissociation of transactivation from transrepression by a selective glucocorticoid receptor agonist leads to separation of therapeutic effects from side effects. *Proc Natl Acad Sci U S A* 2004;101(1):227–32.
- [45] Wu W, Chaudhuri S, Brickley DR, Pang D, Karrison T, Conzen SD. Microarray analysis reveals glucocorticoid-regulated survival genes that are associated with inhibition of apoptosis in breast epithelial cells. *Cancer Res* 2004;64(5):1757–64.
- [46] Stojadinovic O, Lee B, Vouthounis C, Vukelic S, Pastar I, Blumenberg M, et al. Novel genomic effects of glucocorticoids in epidermal keratinocytes: inhibition of apoptosis, interferon-gamma pathway, and wound healing along with promotion of terminal differentiation. *J Biol Chem* 2007;282(6):4021–34.
- [47] Sevilla LM, Bayo P, Latorre V, Sanchis A, Perez P. Glucocorticoid receptor regulates overlapping and differential gene subsets in developing and adult skin. *Mol Endocrinol* 2010;24(11):2166–78.
- [48] Bachelor MA, Cooper SJ, Sikorski ET, Bowden GT. Inhibition of p38 mitogen-activated protein kinase and phosphatidylinositol 3-kinase decreases UVB-induced activator protein-1 and cyclooxygenase-2 in a SKH-1 hairless mouse model. *Mol Cancer Res* 2005;3(2):90–9.
- [49] Wilker E, Lu J, Rho O, Carbajal S, Beltran L, DiGiovanni J. Role of PI3K/Akt signaling in insulin-like growth factor-1 (IGF-1) skin tumor promotion. *Mol Carcinogen* 2005;44(2):137–45.
- [50] Oishi Y, Fu ZW, Ohnuki Y, Kato H, Noguchi T. Molecular basis of the alteration in skin collagen metabolism in response to in vivo dexamethasone treatment: effects on the synthesis of collagen type I and III, collagenase, and tissue inhibitors of metalloproteinases. *Br J Dermatol* 2002;147(5):859–68.
- [51] Fogel AL, Hill S, Teng JC. Advances in the therapeutic use of mammalian target of rapamycin (mTOR) inhibitors in dermatology. *J Am Acad Derm* 2015;72(5):879–89.
- [52] Shi VJ, Levy LL, Choi JN. Cutaneous manifestation of non-targeted and targeted chemotherapies. *Semin Oncol* 2016;43(3):419–25.
- [53] Tan CY, Hagen T. mTORC1 dependent regulation of REDD1 protein stability. *PLoS One* 2013;8(5):e63970.
- [54] Petta I, Dejager L, Ballegeer M, Lievens S, Tavernier J, De Bosscher K, et al. The Interactome of the glucocorticoid receptor and its influence on the actions of glucocorticoids in combatting inflammatory and infectious diseases. *Microbiol Mol Biol Rev* 2016;80(2):495–522.
- [55] Vandevyver S, Dejager L, Tuckermann J, Libert C. New insights into the anti-inflammatory mechanisms of glucocorticoids: an emerging role for glucocorticoid-receptor-mediated transactivation. *Endocrinology* 2013;154(3):993–1007.
- [56] Beato M, Herrlich P, Schutz G. Steroid hormone receptors: many actors in search of a plot. *Cell* 1995;83(6):851–7.
- [57] Chen W, Dang T, Blind RD, et al. Glucocorticoid receptor phosphorylation differentially affects target gene expression. *Mol Endocrinol* 2008;22(8):1754–66.
- [58] Ismaili N, Garabedian MJ. Modulation of glucocorticoid receptor function via phosphorylation. *Ann N Y Acad Sci* 2004;1024:86–101.
- [59] Galliher-Beckley AJ, Cidlowski JA. Emerging roles of glucocorticoid receptor phosphorylation in modulating glucocorticoid hormone action in health and disease. *IUBMB Life* 2009;61(10):979–86.
- [60] Oakley RH, Cidlowski JA. The biology of the glucocorticoid receptor: new signaling mechanisms in health and disease. *J Allergy Clin Immunol* 2013;132(5):1033–44.
- [61] Del Rosso J, Friedlander SF. Corticosteroids: options in the era of steroid-sparing therapy. *J Am Acad Dermatol* 2005;53(1S1):S50–8.
- [62] Kumar S, Goyal A, Gupta YK. Abuse of topical corticosteroids in India: concerns and the way forward. *J Pharmacol Pharmacother* 2016;7(1):1–5.
- [63] Vandewalle J, Luypaert A, De Bosscher K, Libert C. Therapeutic mechanisms of glucocorticoids. *Trends Endocrinol Metab* 2018;29(1):42–54.
- [64] Wang H, Kubica N, Ellisen LW, Jefferson LS, Kimball SR. Dexamethasone represses signaling through the mammalian target of rapamycin in muscle cells by enhancing expression of REDD1. *J Biol Chem* 2006;281(51):39128–34.
- [65] Henneicke H, Gasparini SJ, Brennan-Speranza TC, Zhou H, Seibel MJ. Glucocorticoids and bone: local effects and systemic implications. *Trends Endocrinol Metab* 2014;25(4):197–211.